Crystallisation kinetics and magnetic properties of a Co-based amorphous alloy

S. Lesz [a,*], R. Nowosielski [a], B. Kostrubiec [b], Z. Stokłosa [b]

[a] Division of Nanocrystalline and Functional Materials and Sustainable
Pro-ecological Technologies, Institute of Engineering Materials and Biomaterials,
Silesian University of Technology, ul. Konarskiego 18a, 44-100 Gliwice, Poland
[b] Institute of Materials Science, Silesian University, Bankowa 12, 40-007 Katowice, Poland
* Corresponding author: E-mail address: sabina.lesz@polsl.pl

Materials

ABSTRACT

Purpose: In the present paper, the kinetics of crystallization process and its correlation with magnetic properties of the $Co_{80}Si_9B_{11}$ alloy was carefully examined.

Design/methodology/approach: The following experimental techniques were used: X-ray diffraction (XRD), electrical resistivity in situ measurements (four-point probe), saturation magnetization in situ measurements (magnetic balance) and initial relative magnetic permeability measurements (Maxwell-Wien bridge).

Findings: The investigations proved that thermal annealing of amorphous $Co_{80}Si_9B_{11}$ alloy leads to a crystallization process and radical changes of magnetic properties. The activation energy of this process was determined as E_c=3.0±0.2 eV.

Research limitations/implications: According to the results presented in the present paper the examined alloys can be used as a very good soft magnetic material.

Originality/value: The best soft magnetic properties are observed in as quenched state.

Keywords: Amorphous and nanocrystalline alloys; Heat treatment annealing; Magnetic properties; X-ray diffraction method

1. Introduction

The transition metal-metaloid amorphous alloys described in general as $TL_{1-x}M_x$, where TL=Fe, Co or Ni and M=B, Si, C, N, P, Ge, represent an important class of materials with both scientific and technological unique material properties. This class of materials exhibit excellent soft magnetic properties such as low coercivity and hysteresis loss and high permeability, which render the alloys to be an outstanding candidate for host of applications including electronics, magnetic recording heads, magnetic sensors and large transformers and electronic devices [1÷4]. Alloys of the binary Co-B system can easily be amorphized by melt spinning. More complex alloys with specific properties can be obtained by adding other elements to this system [5÷10] and various chemical compounds can be crystallized from the amorphous phase at specific temperatures. It is generally known that good soft magnetic properties of melt-spun amorphous alloys are lost by annealing-induced crystallization [4]. However, in the last decade, an increase in soft magnetic properties has been reported in a number of multi-phase nanocrystalline Fe-based amorphous alloys [11÷16]. Hence, the kinetics of crystallization of an amorphous system is a key subject for study, since it provides new opportunities for structure control by innovative alloy design and processing techniques. The kinetics of crystallization of amorphous alloys is often described by the well-known phenomenological Johnson-Mehl-Avrami equation for isothermal experiments [17, 18]. The activation energy of the crystallization process can be obtained from the temperature dependence of the reaction-rate constant, which is known as Kissinger's method [17, 19].

The crystallization kinetics of Co-based amorphous alloys is scarcely studied while substantial amount of work exists on those of Fe-based amorphous alloys. Therefore, it is necessary to study the crystallization kinetics connecting with magnetic properties of alloy. In the present work both crystallization kinetics and magnetic properties of Co-Si-B alloy are investigated.

2. Experiments

An amorphous alloy ribbons with composition $Co_{80}Si_9B_{11}$ were prepared by a planar flow casting method. Typical samples produced were 0.014 mm thick and 7 mm wide. Composition of samples was verified by X-ray fluorescence (XRF) using the SUPERPROBE 733 JEOL.

Sections of ribbons of 110 mm length were annealed in electric chamber furnace THERMOLYNE type F6020C with protective argon atmosphere in the temperature range from 373÷873 K with step of 50 K. The annealing time was constant and equal to 1 h.

The structure investigations have been performed by X-ray diffraction (XRD) method using diffractometer XRD7, SEIFERT-FPM. Crystalline phases were identified by XRD using filtered Co-K_α radiation.

Magnetic measurements of samples in as quenched state and after annealing in temperature range T_a= 373÷873 K, have been done. The following magnetic properties were measured: initial relative magnetic permeability μ_r with the use of Maxwell-Wien bridge (at frequency about 1 kHz and magnetic field =0.5 A/m) and saturation magnetization J with the use of magnetic balance. Measurements of saturation magnetization J were performed for the samples in as quenched state however initial relative magnetic permeability μ_r was performed for samples in as quenched state as well as after annealing.

Kinetics of the crystallization process was examined by applying two experimental techniques: electrical resistivity measurements in situ with different heating rates in the range 0.5÷4.4 K/min and measurements of saturation magnetization as a function of temperature $M(T)$. From the isochronous resistivity curve of the investigated alloy the crystallization temperature T_{x1} of the amorphous alloy and the effective activation energy for the crystallization E_c were determined. The crystallization temperature T_{x1} of samples can be obtained from the condition $d\rho/dT$=0. For analyzed samples the linear heating rate was equal to 0.5 K/min [17]. The effective activation energy for the crystallization E_c was evaluated by the Kissinger method [17, 19], which is written as Eq. (1):

$$\ln \frac{V_l}{T_h^2} + \ln const = -\frac{E_c}{k_B} \cdot \frac{1}{T_h} \qquad (1)$$

where: E_c, is the effective activation energy for the crystallization processes, V_l, is linear heating rate, T_h – is the so-called temperature of an homological point determined for the heating rate V_l, i.e. temperature which the rate of crystallization process is maximum [17], and k_B is the Boltzman constant.

Measurements of saturation magnetization of samples were used. Samples in as quenched state were heated with heating rates: 5 and 10 K/min up to 1000 K, and simultaneously, $M(T)$ curves were recorded by applying magnetic balance technique. The results were presented as normalized curves $M(T)/M$(300 K).

3. Results and discussion

It was found from the obtained results of structural studies performed by X-ray diffraction that in as quenched state the $Co_{80}Si_9B_{11}$ alloy has amorphous structure (Fig. 1). Only a broad diffraction peak at about $2\Theta \cong 52°$ can be observed from Fig. 1, indicating that obtained ribbon had amorphous structure.

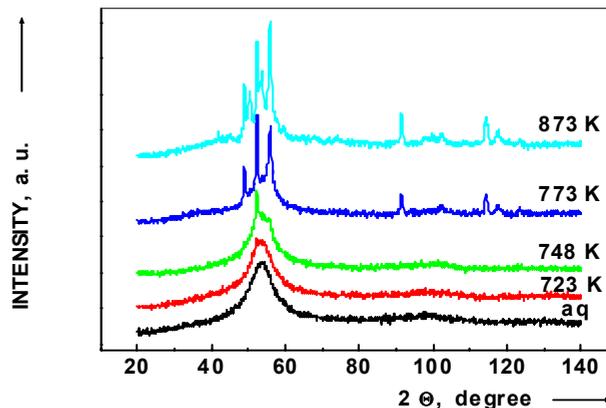Fig. 1. X-ray diffraction pattern of the $Co_{80}Si_9B_{11}$ alloy in as quenched state and after annealing in temperature range 723÷873K

The investigated $Co_{80}Si_9B_{11}$ alloy in as quenched state has a high value of resistivity ρ equal 1.15 $\mu\Omega$m (Fig. 2) and the following magnetic properties: saturation magnetization J_S= 0.8 T (Fig. 3) and initial relative magnetic permeability μ_r =1450 (Fig. 4). The obtained physical properties, i.e. ρ, J_s, and μ_r allow to classify the $Co_{80}Si_9B_{11}$ alloy in as quenched state as a soft magnetic material.

On the basis of isochronous curves of electric resistivity ρ as function of annealing temperature T, it was found that conventional crystallization temperature (usually obtained for the heating rate 0.5 K/min [10]) T_{x1} was equal 655 K (Fig. 2). The temperature T_{x1} is shifted towards higher temperatures with an increase of the heating rate (Fig. 2). This suggests that the crystallization process of the amorphous $Co_{80}Si_9B_{11}$ alloy should be considered as thermally activated process [4].

Using the Kissinger method the effective activation energy of crystallization E_c was determined. The results achieved from isochronous curves of electric resistivity in the co-ordinate system $\ln(v/T_h)$ versus T_h^{-1} have been shown in Fig. 5. The effective activation energy of the crystallization process determined from the slope of the straight line (according to equation (1)) is 3.0±0.2 eV.

Fig. 6 shows normalized in situ curves of magnetization for the alloy. This figure shows that the beginning of the crystallization process takes place at 725 K (for the heating rate 5 K/min). X-ray diffraction measurements indicate that initially the hexagonal (h.c.p.) α-Co phase is formed and subsequently the boride Co_3B is formed at 773 K (Fig. 1, Table 1).

The worked out investigations at temperature annealing in range 373÷873 K by 1 h of the investigated alloy have showed that in mentioned temperature range, the changes of structure and magnetic properties took place (Fig. 1, 2, 4, 6, Table 1). Fig. 1 shows the XRD data obtained from the $Co_{80}Si_9B_{11}$ alloy ribbons from 723÷873 K. From Fig. 1 can be seen, that the diffraction

patterns of the $Co_{80}Si_9B_{11}$ alloy annealed from 723÷748 K are almost the same as in as quenched state. Increase of the annealing temperature above 723 K leads to changes of structure of the investigated alloy (Fig. 1). As can be seen from Fig. 1, at 748 K the bulk crystallization of the amorphous alloy proceeds through nucleation of the hexagonal (h.c.p.) α-Co phase in the amorphous matrix. Further increase of the annealing temperature leads to change in the X-ray diffraction pattern (Fig. 1) and at T_a=773 K in addition to the α-Co phase, orthorhombic Co_3B phase was identified. However on X-ray diffraction pattern for ribbons annealed at temperature T_a=873 K the existence of Co_2B and Co_2Si together with α-Co and Co_3B phases were observed (Fig. 1, Table 1). Similar structural changes were found for $Co_{70}Si_{12}B_{18}$ and $Co_{78}Si_{11}B_{11}$ alloys studied by electrical conductivity and thermal expansion measurements [20, 21].

Fig. 4. The initial relative magnetic permeability μ_r measured at room temperature for $Co_{80}Si_9B_{11}$ alloy after 1 h annealing at temperature T_a
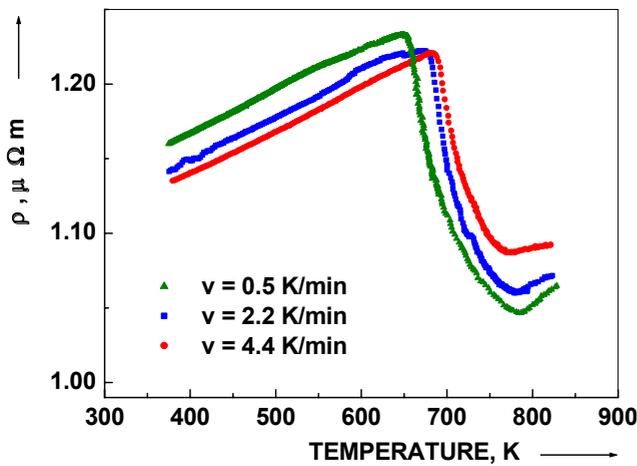

Fig. 2. The in situ isochronal resistivity curves for $Co_{80}Si_9B_{11}$ alloy obtained with heating rate 0.5, 2.2 and 4.4 K/min

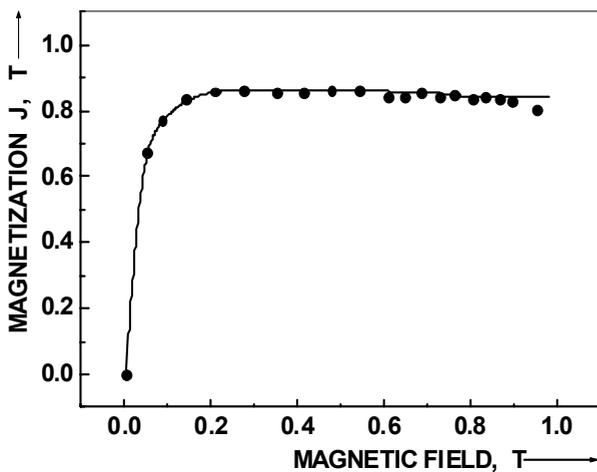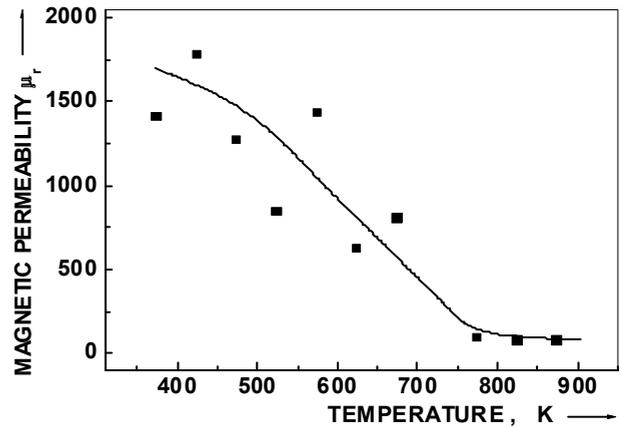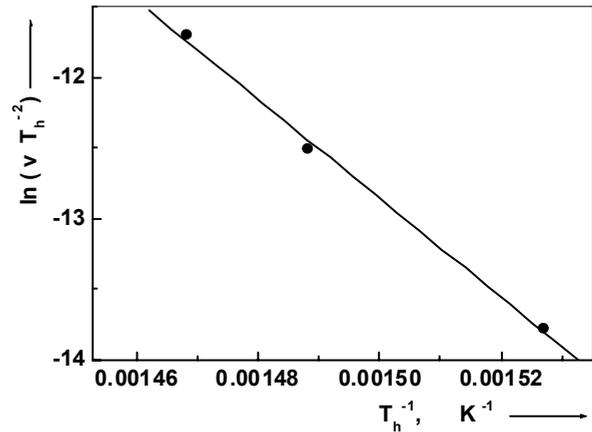Fig. 5. Plot of $\ln(v/T_h^2)$ versus T_h^{-1} for $Co_{80}Si_9B_{11}$ alloy

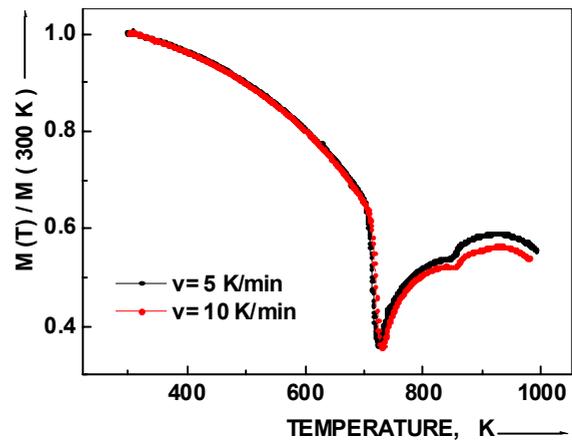Fig. 3. Magnetization J versus magnetic field for $Co_{80}Si_9B_{11}$ alloy obtained by magnetic balance

Fig. 6. Normalized magnetization versus temperature T of $Co_{80}Si_9B_{11}$ alloy

Table 1.
The phase analysis results for the $Co_{80}Si_9B_{11}$ alloy annealed at T_a=773 and 873 K (see Fig. 1)

d, Å	d $_\alpha$ (hkl) for phases:			
	α-Co	Co_3B	Co_2B	Co_2Si
2.500				2.510 (200)
2.340		2.363 (112)		
2.165*	2.165 (100)			
2.130		2.128 (121)		2.130 (310)
2.100			2.113 (002)	
2.030*	2.023 (002)	2.031 (210)		2.020 (220)
2.000				2.000 (301)
1.980		1.975 (103)	1.983 (211)	1.970 (121)
1.940*		1.942 (211)		
1.910*	1.910 (101)			
1.870		1.860 (122)		1.870 (002)
1.850		1.848 (113)		1.850 (311)
1.800			1.815 (112)	
1.740		1.732 (212)		
1.700				1.700 (112)
1.660*		1.657 (004)		1.670 (410)
1.616		1.620 (130)	1.616 (202)	
1.590			1.588 (310)	1.600 (130)
1.485	1.480 (102)			
1.250*	1.252 (110)			1.250 (412)
1.187			1.192 (213)	1.190 (113)
1.179			1.183 (330)	
1.167			1.169 (411)	
1.149*	1.149 (103)			
1.105				1.110 (023)
1.101				1.100 (512)
1.083	1.083 (200)			
1.065*	1.066 (112)			
1.046*	1.047 (201)			1.050 (341)
1.031				1.032 (332)
1.016*	1.015 (004)			
0.987			0.973 (204)	

d – lattice parameters calculated from Fig. 1
d$_\alpha$ – lattice parameters of identified phases [22]
* - the peak appearing in $Co_{80}Si_9B_{11}$ alloy annealed at T_a=773 K, too

Fig. 4 shows the initial magnetic permeability μ_r measured as a function of annealing temperature T_a. From Fig. 4 it can be recognized that for the $Co_{80}Si_9B_{11}$ alloy annealed in temperature range from 373÷723 K the initial magnetic permeability μ_r has high value i.e. 1420÷1090. The further increase of temperature annealing T_a leads to significant decrease of the μ_r and is connected with formation of borides in the investigated alloy.

Described process of crystallization based on analysis of isochronous electrical resistivity curve exhibits in general the correlation between proceeding of alloy crystallization determined in X-ray diffraction method and magnetic properties.

4. Conclusions

The research showed that $Co_{80}Si_9B_{11}$ alloy in as quenched state has an amorphous structure and the following physical properties: electrical resistivity ρ equal 1.15 μΩm, saturation magnetization J_S=0.8 T and initial relative magnetic permeability μ_r=1460.

The investigations proved that thermal annealing of amorphous $Co_{80}Si_9B_{11}$ alloy within the temperature range 373÷873 K leads to a crystallization process and radical changes of magnetic properties.

The effective activation energy E_c for the crystallization process is (3.0±0.2) eV. This value is higher than the one of alloys with similar chemical compositions [23]. This indicates that $Co_{80}Si_9B_{11}$ amorphous alloy exhibits much higher thermal stability against crystallization.

The crystallization process of $Co_{80}Si_9B_{11}$ alloy is connected with the formation of the hexagonal (h.c.p.) α-Co phase in an amorphous matrix at the temperature T_{x1} called the temperature of the first stage of the crystallization process, and with appearance of boride phases at the second stage of the crystallization process of $Co_{80}Si_9B_{11}$ alloy. The conventional crystalllization temperature T_{x1} of $Co_{80}Si_9B_{11}$ alloy, determined from in situ isochronous resistivity curves (the heating rate of 0.5 K/min) is 655 K.

The temperature of the second stage of crystallization (T_{x2}≅773 K) of the investigated alloy, connected with the appearance of the boride phase, was determined by both methods: the XRD and measurements of magnetization in saturation [24]. The existence of boride phases in $Co_{80}Si_9B_{11}$ alloy was confirmed by a dramatical decrease of initial magnetic permeability μ_r after annealing of the samples within 773÷873 K.

References

[1] I.C. Rho, C.S. Yoon, C. K. Kim, T.Y. Byun, K.S. Hong: J. Non-Cryst. Solods 316 (2003) 289.

[2] G. Buttino, A. Cecchetti, M. Poppi: J. Magn. Magn. Mater. 241 (2002) 183.

[3] I.C. Rho, C. S. Yoon, C. K. Kim, T. Y. Byun, K. S. Hong: Mater. Sci. Eng. B96 (2002) 48.

[4] Z.Z. Yuan, X. D. Chen, B. X. Wang, Z.J. Chen: J. Alloys Comp. 399 (2005) 166.

[5] H. Beck, H. J. Guntherodt: Glassy Metals II, Atomic Structure and Dynamics, Electronic Structure, Magnetic Properties, 1983.

[6] S. Mudry, B. Kotur, L. Bednarska, Y. Kulyk, A. Korolyshyn, O. Heretyk: J. Alloys Comp. 367 (2004) 274.

[7] L.A. Dobrzański, R. Nowosielski, J. Konieczny, A. Przybył: J. Mater. Proc. Techn. 162-163 (2005) 20.

[8] J. Konieczny L.A. Dobrzański, R. Nowosielski, J. Wysłocki, A. Przybył: Proc. of the Third Scientific Conference „Materials Mechanical and Manufacturing Engineering MMME'05" Gliwice-Wisła (2005) 249.

[9] L.A. Dobrzański, R. Nowosielski, J. Konieczny: J. Mater. Proc. Techn. 155-156 (2004) 1943.

[10] L.A. Dobrzański, R. Nowosielski, J. Konieczny, J. Wysłocki, A. Przybył: J. Mater. Proc. Techn. 157-158 (2004) 669.

[11] S. Lesz, R. Szewczyk, D. Szewieczek, A. Bieńkowski: J. Mater. Proc. Techn. 157-158 (2004) 743.

[12] D. Szewieczek, S. Lesz: J. Mater. Proc. Techn. 162-163 (2005) 254.

S. Lesz, R. Nowosielski, B. Kostrubiec, Z. Stokłosa,

[13] M. E. McHenry, M. A. Willard, D. E. Laughlin: Progress in Mater. Sci. 44 (1999) 291.

[14] S. Lesz, D. Szewieczek: Proc. of the Worldwide Congress on Materials and Manufacturing Engineering and Technology COMMENT'2005, Poland, Gliwice-Wisła, 16-19th May (2005) (CD-ROM) 637.

[15] D. Szewieczek, S. Lesz: Proc. of the 13th International Scientific Conference „Achievements in Mechanical & Materials Engineering AMME'05" Gliwice-Wisła (2005) 637.

[16] D. Szewieczek, S. Lesz: J. Mater. Proc. Techn. 157-158, (2004) 771.

[17] J. Rasek: Some diffusion phenomena in crystalline and amorphous metals, Silesian University Press, Katowice (2000). (in Polish)

[18] P. Kwapuliński, A. Chrobak, G. Haneczok, Z. Stokłosa, J. Rasek, J. Lelątko: Mater. Sci. Eng. C 23 (2003) 71.

[19] H. E. Kissinger: Anal. Chem. 29 (1957) 1702.

[20] L. T. Baczewski, P. Duhaj, P. Svec, G. Vlasak: Acta Phys. Pol. A 72 (1987) 125.

[21] D. Dróżdż, T. Kulik: Inżynieria Materiałowa 4 (2001) 283.

[22] R. Jenkins, W.F. McClune, T.M. Maguire, et al.: Powder Diffraction Data, JCPDS – International Centre for Diffraction Data, 1601 Parklane, Swarthmore, PA 19081, USA, 1986.

[23] P. Vojtaník, J. Kravčák, R. Varga: J. Magn. Magn. Mater. 157/158 (1996) 175.

[24] C.S. Yoo, S.K. Lim, C.S. Yoon, C.K. Kim: J. Alloys Comp. 359 (2003) 261.